International Journal of Remote Sensing
Vol. 000, No. 000, Month 2005, 1–16

Taylor & Francis
Taylor & Francis Group

Urban vegetation monitoring in Hong Kong using high resolution multispectral images

J. NICHOL* and C. M. LEE

Department of Land Surveying and Geo-Informatics, The Hong Kong Polytechnic University, Kowloon, Hong Kong

(*Received 31 October 2003; in final form 1 June 2004*)

Very high resolution (VHR) satellite remote sensing systems are now capable of providing imagery with similar spatial detail to aerial photography, but with superior spectral information. This research investigates the hypothesis that it should be possible to use multispectral IKONOS images to quantify urban vegetation, obtaining similar accuracy to that achieved from false colour aerial photographs. Two parameters, vegetation cover and vegetation density are used to represent biomass in the study area (Kowloon, Hong Kong), for which data is collected for 41 field quadrats. Regression equations relating the field measurements of vegetation density to image wavebands obtained similar high correlations for both image types and lower but significant correlations for vegetation cover. Vegetation density is a quantifiable measure of vegetation in multiple layers above ground, representing the total amount of biomass and is thus well able to indicate the diverse structural types of vegetation found in urban areas. Furthermore it can be accurately measured using the IKONOS green/red ratio (Chlorophyll Index). The superiority of the latter to the more commonly used Normalized Difference Vegetation Index (NDVI), is attributed to the sub-optimal timing of the imagery during the dry season, and its greater sensitivity to multiple layering within the vegetation canopy. A time and cost comparison between the two image types suggests that the use of IKONOS images is much more cost effective than aerial photographs for urban vegetation monitoring.

1. Introduction

Conventional methods of mapping urban vegetation combine colour infrared aerial images and fieldwork, since medium resolution satellite images used in urban areas such as Satellite pour l'Observation de la Terre (SPOT) (Barnsley and Barr 1996) and Landsat (Gao and Skillcorn 1998) lack the necessary spatial detail to detect the often fragmented vegetation cover such as a single row of street trees or a grassy road verge. Since aerial photographs are not digital, manual interpretation has remained the preferred tool of planners in much of the world and developing countries for inventorying the urban forest. The techniques are described by Nowak *et al.* (1996). However, the limited coverage of a single air photograph and the difficulty of integrating air photographs to produce city-wide vegetation maps suggests that the new generation of fine resolution satellite sensors should be investigated for their wider coverage. Even in developed countries where digital videography is becoming a relatively inexpensive digital alternative to air

*Corresponding author. Email: lsjanet@polyu.edu.hk

International Journal of Remote Sensing
ISSN 0143-1161 print/ISSN 1366-5901 online
http://www.tandf.co.uk/journals
DOI: 10.1080/01431160412331291198

photographs, the ability to obtain regular multispectral images from the same sensor, calibrated to absolute radiance or reflectance values, makes space-borne systems a competitive option.

This study evaluates the effectiveness of multispectral IKONOS satellite images, in comparison with digitized colour infrared aerial photographs, for measuring both the extent and total amount of green biomass in a densely urbanized area of central Kowloon on Hong Kong's mainland. The spectral and spatial resolution of each sensor type is evaluated in the context of the main objectives, namely, to test

(i) whether urban vegetation can be accurately measured using automated multispectral remote sensing;
(ii) whether multispectral IKONOS images are more cost-effective than false colour aerial photographs for representing urban vegetation;
(iii) which of the field measured parameters vegetation cover or vegetation density provide the most accurate model of biomass recorded on very high resolution (VHR) images;
(iv) the effectiveness of single wavebands for modelling biomass;
(v) the effectiveness of the ratio-based vegetation indices Normalized Difference Vegetation Index (NDVI) (Tucker 1979) and Chlorophyll Index (Kanemasu 1974) for modelling urban biomass;
(vi) methods for the removal of tree crown shadows from the images in order to better model the ground vegetation.

Only single band and band ratio-based indices were considered in this study since perpendicular indices are more sensitive to soils than ratio-based indices (Lawrence and Ripple 1998). Thus the wide variety of vegetation backgrounds in urban areas, including wet and dry soil, concrete, asphalt, brick and tile, would reduce the ability of perpendicular indices to distinguish differences in vegetation cover. Of the ratio-based indices, the NDVI and Chlorophyll Index were selected, the former for its robustness and common usage and the latter because it is a ratio of the green and red wavelengths and initial results showed that the green and red bands alone gave high correlations with vegetation in the study area. Moreover, it was hypothesized that the Chlorophyll Index should provide a better measure than NDVI in urban areas because, according to Colwell (1974), when the background is light and leaf area is low, the negative relationship between Leaf Area Index (LAI) and the red wavelengths may be stronger than the positive relationship between the LAI and the near-infrared (NIR) wavelengths, because both the vegetation and background are highly reflecting in the NIR region.

2. Images used

Summer images are rarely obtained in this sub-tropical region due to high cloud cover. This study used a pair of aerial photographs acquired by the Hong Kong Lands Department on 25 October 2002 using Kodak IR443 film with a nominal photograph scale of 1 : 8000. The photograph diapositive was scanned to a ground resolution of 0.5 m, giving three 8-bit bands (a 16-bit scanner was not available) corresponding to green, red and infrared portions of the spectrum (table 1).

A multispectral IKONOS image of 23 November, 2000, having a spatial resolution of 4 m in four 11-bit wavebands, and with an off-nadir look angle of 19° (table 1) was used for the study. It covers the whole of Kowloon Peninsula and the

105983
International Journal of Remote Sensing res50633.3d 2/11/04 14:07:19
The Charlesworth Group, Wakefield +44(0)1924 369598 - Rev 7.51n/W (Jan 20 2003)

Table 1. Details of images used.

Item	Infrared aerial photographs	IKONOS image
Image date	25 October 2002	23 November 2000
GIFOV	0.5 m	4 m
Spectral response function	Band 1 green	Band 1 blue 0.45–0.52
	Band 2 red	Band 2 green 0.52–0.6
	Band 3 near-infrared (NIR)	Band 3 red 0.63–0.69
		Band 4 NIR 0.76–0.9
Radiometric resolution	Scanned at 8 bits	11 bits
Solar zenith angle (°)	27 (11.50 am)	44 (11 am)
Image scene size	2 km × 2 km	11 km × 11 km
View zenith (°)	Near nadir	19 off nadir
Scene centre latitude longitude	114°11 E, 22°18 N	114°16 E, 22°30 N

105983
International Journal of Remote Sensing res50633.3d 2/11/04 14:07:19
The Charlesworth Group, Wakefield +44(0)1924 369598 - Rev 7.51n/W (Jan 20 2003)

northern part of Hong Kong Island (figure 1). The two-year time difference between the air photographs and the IKONOS image does not preclude comparison since they both correspond to Hong Kong's winter and dry season. The biomass changes little inter-annually due to regular cutting and management, and the study area is a mature built-up area with few land cover changes. Geometric correction to the Hong Kong Grid coordinate system using a cubic order polynomial was performed for the air photographs and IKONOS image respectively, to enable them to be aligned with infrastructural features and global positioning system (GPS) readings during fieldwork. A root-mean-square (RMS) error of 8.3 pixels (4.15 m) and 1.4 pixels (5.6 m) was obtained for the air photographs and IKONOS image,

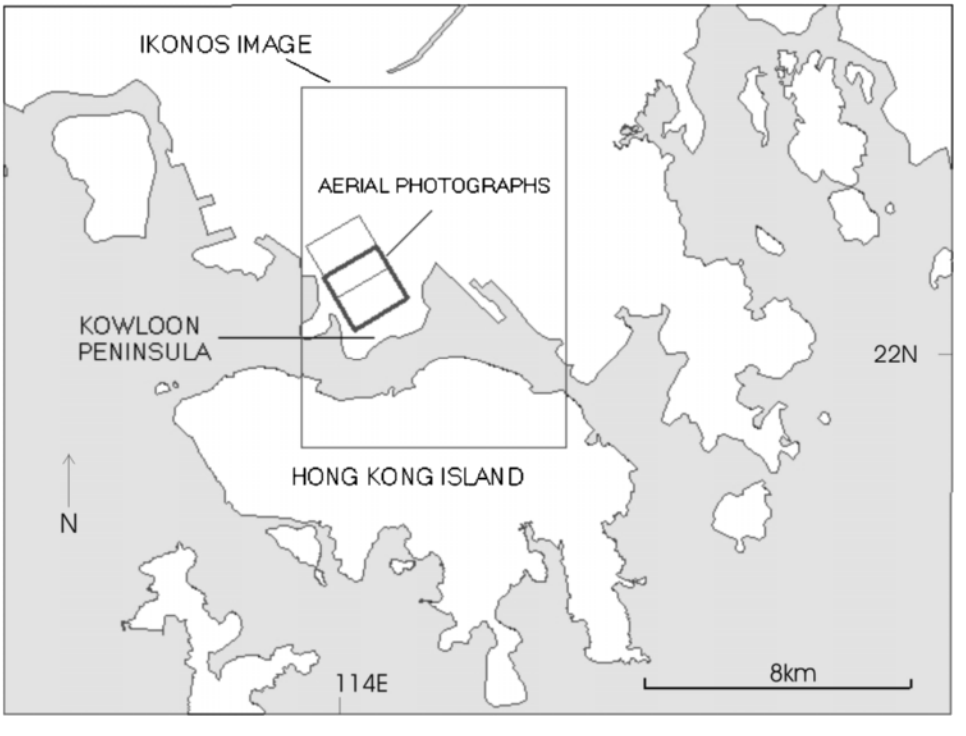

Figure 1. Location of aerial photographs and the IKONOS image in the study area.

respectively. This relatively large error is due to the off-nadir look angle in the case of IKONOS, and the inherent distortion of aerial photographs due to platform instability. However this error was taken into consideration as a parameter when determining the sizes of sample plots (G in equation (2)). Additionally most of the field sampling plots were homogeneous in nature, and care was taken not to locate them near the habitat edge.

3. Image conversion

Because the Normalized Difference Vegetation Index (NDVI) is known to be a robust indicator of green vegetation (Tucker 1979) NDVI images were generated using the red and NIR bands of both the air photographs and the IKONOS image. In the case of IKONOS NDVI, since it comprises two bands, each with a different slope calibration to the digital number (DN) value, the images were converted to radiance using the gains and offsets given by Fleming (2003) before computing the ratio images. This gave a result comparable with NDVI from other sensors. However, DN was used for comparing individual bands with biomass. Atmospheric correction was not necessary for the air photographs flown at 4000 ft, but for the IKONOS image it was required in order to compensate for the differential effects of Rayleigh scattering in the ratioed bands. It was performed using the dark pixel subtraction method (Chavez 1988) with the darkest image pixel found from the image histograms. However this calculation does not account for changes in radiance due to aerosols or atmospheric absorption, and thus departs from more typical calculations of NDVI that use apparent reflectance.

3.1 *Normalization of air photograph bands to IKONOS wavebands*

Since the spectral ranges of the air photograph bands green, red and infrared do not give absolute radiance measurements, a relative radiometric correction technique using IKONOS as the reference was adopted, to normalize the air photograph wavebands using the darkest and lightest target pixels in each band to develop a regression equation (equation (1)) (Hall *et al.* 1991). This was done within the area covered by both the air photographs and the IKONOS image. The method is only approximate since the relationship between film exposure and photographic tone in each band cannot be assumed to be linear.

$$Y = m(\mathrm{DN} + b) \tag{1}$$

where $m=(B_r-D_r)/(B_s-D_s)$, $b=(D_r(B_s-D_s)(B_r)/(B_s-D_s)$. Y=subject image, DN=digital number of the subject image, B_r=mean digital number for the bright target of the reference image, B_s=mean digital number for the bright target of the subject image, D_r=mean digital number for the dark target of the reference image, D_s=mean digital number for the dark target of the subject image.

4. The study area and field sampling strategy

The central part of Kowloon Peninsula (figure 1) was selected for the study area as it typifies urban Hong Kong, with a dense living environment containing moderate, but variable amounts and types of vegetation. Since most buildings are high rise, streets are often obscured by shadow on the images. Vegetation varies from short grass cover on sports pitches through tall grass and shrubby cover on waste ground, to residual primary forest on a steeply sloping inselberg. The size of each sample site

105983
International Journal of Remote Sensing res50633.3d 2/11/04 14:07:20
The Charlesworth Group, Wakefield +44(0)1924 369598 - Rev 7.51n/W (Jan 20 2003)

was selected according to the formula in equation (2) (Justice and Townsend 1981) which considers the Ground Instantaneous Field of View (GIFOV) and geometric accuracy of the images, the latter being derived from the RMS error of the georeferencing process.

$$A = (P(1+2G)) \tag{2}$$

where A=size of area to be sampled, P=GIFOV G=geometric accuracy of the image (in number of pixels). The recommended minimum sample sizes for IKONOS and the aerial photographs were 15.6 m^2 and 6.1 m^2, respectively. The larger plot size of 16 m^2 was selected.

The aerial photographs were used to locate 41 sample plots, which were used to derive a regression equation describing the empirical relationship between biomass and image radiance. For ground sampling, the line intercept method (Hanley 1978) was used as being faster than measuring the whole plot, but with comparably high accuracy. Five parallel sampling lines with 4 m separation between them provided baselines along each of which two parameters, vegetation cover (VC) and vegetation density (VD) were measured. VC was estimated according to equations (3) and (4).

$$\%\ \mathrm{VC} = 100(1 - LV/TL) \tag{3}$$

where LV=length covered by vegetation type x, TL=total length in plot (80 m).

Since vegetation cover only estimates the proportion of the line intercepted by vegetation it does not record the leaf overlap and does not account for multiple layers of vegetation. It records the same value for all structural types including grass, shrubs and trees and therefore is not a biomass indicator. It is synonymous with the vegetation fraction (VF) of Gitelson *et al.* (2002). However reflectance from a vegetation canopy originates from all layers of vegetation (Suits 1972) and the environmental importance of vegetation in urban areas is related to the total amount of biomass. Therefore a second parameter, vegetation density was devised to measure vegetation amount in all vertical layers above ground. This parameter was devised by the authors to represent the amount of green biomass as a substitute for the commonly used LAI (Curran 1983) which is defined as the cumulative, one-sided leaf area per unit ground area. LAI could not be collected since it requires either harvesting of the vegetation or electronic equipment, which was not available. Vegetation density was computed according to equation (4), with weightings (W) given in table 2.

$$\%\ \mathrm{VD} = 100\Sigma((W\,LV_x)/TL)/SW \tag{4}$$

where: x=vegetation types 1–5 (table 2), W=weighting for vegetation type x LV=length covered by vegetation type x TL=total length in plot (80 m), SW=sum of weightings (2.1).

Table 2. Weightings allocated to structural vegetation types for vegetation density.

Class	Weighting	Description
1. Short grass	0.2	Green grass lower than 0.5 m
2. Tall grass	0.3	Green grass higher than 0.5 m
3. Shrub	0.4	Short and woody plant with woody (non-green) stems from the base
4. Small tree	0.5	Woody plant with trunk diameter less than 0.3 m
5. Large tree	0.7	Woody plant with trunk diameter greater than 0.3 m

Weightings were allocated approximately according to mean relative values of LAI for grassland, shrub and forest biomass given in Scurlock *et al.* (2001), and adjusted to accommodate two categories of grass and two tree sizes as observed in the study area.

Thus VD differs from vegetation cover (VC), which represents the percentage of ground covered by vegetation. For example, all vegetated areas have a value for both VC and VD but the value for VD may be much lower. Thus a football pitch with a complete cover of short grass (VC=100%) would have a VD value of only 9.5%, but a fairly well vegetated forest plot having 90% cover of tall trees, 30% shrub and 10% tall grass (with VC of 90–100%) would have a VD value of 45% (table 3).

The coordinates of the sample plots were recorded in the field using a GPS and overlaid onto the images. The image statistics and correlation coefficients R and R^2 were then derived for different combinations of image bands to analyse the relationship between image bands and ground measured biomass (vegetation cover and vegetation density). The polynomial regressed images that achieved the highest correlations were further processed for shadow removal. Images of VD and VC (figure 2) were generated from these following shadow removal, using the regression equations.

105983
International Journal of Remote Sensing res50633.3d 2/11/04 14:07:20
The Charlesworth Group, Wakefield +44(0)1924 369598 - Rev 7.51n/W (Jan 20 2003)

Table 3. Comparison of values recorded for two vegetation parameters.

Vegetation types in plot	VC (%)	VD (%)
Well vegetated: 90% tall tree, 30% shrub, 10% grass	90–100	43
Football pitch: 100% short grass	100	9.5
Waste ground: 30% shrub, 40% grass	40–70	14
Street tree, crown occupying full pixel: 100% tall tree	100	33

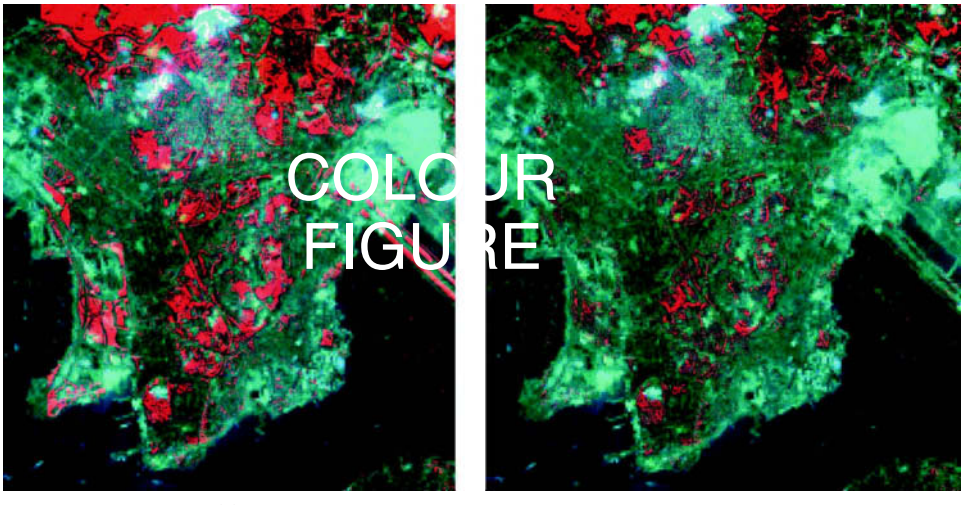

(*a*) (*b*)

Figure 2. False colour composite of VD and VC combining Landsat ETM+ bands 2 and 3 on blue and green, and IKONOS VD and VC on red display. (*a*) Vegetation cover (VC) represents a range of biomass amount and displays as a range of pink to red; (*b*) vegetation density (VD), which records only presence or absence, displays as bright red.

5. Shadow removal

Shadows cast by tall objects comprise a significant component of VHR images and in the study area the shadows of buildings and trees comprise approximately 20% and 10% respectively of the image area, obscuring ground detail. For example, a solar zenith angle of 44° at the image time means that a tree 3 m tall casts a shadow of 3 m and a building 35 m tall casts a shadow of 34 m. In Hong Kong, high rise and high density building means that the inter-building space is often shorter than the shadow length and features within street canyons are obscured. Building shadow is most likely to be obscuring other buildings and streets but most of the tree shadow falls within the tree canopy itself due to multiple layering, rather than on the ground adjacent to the trees and it is spectrally separable from building shadow in the NDVI band (figure 3).

Since the air photographs and the IKONOS image were acquired with different solar geometries, shadow removal was a prerequisite for direct comparison of the two image types. Two approaches to shadow removal were tested. The first was to calculate the mean of the image pixels for each plot, ignoring the shadow pixels by assigning them either a null value, or the mean value of the sample plot. This would increase the mean NDVI values for the plots a little, but the results would not represent the actual ground situation. The second approach is to replace the shadow pixel values with the values of the most likely cover type. In the case of tree canopy shadows this is tree crown, since the shadows are mainly due to multiple layering within the canopy and for building shadow this is built areas. This correction was

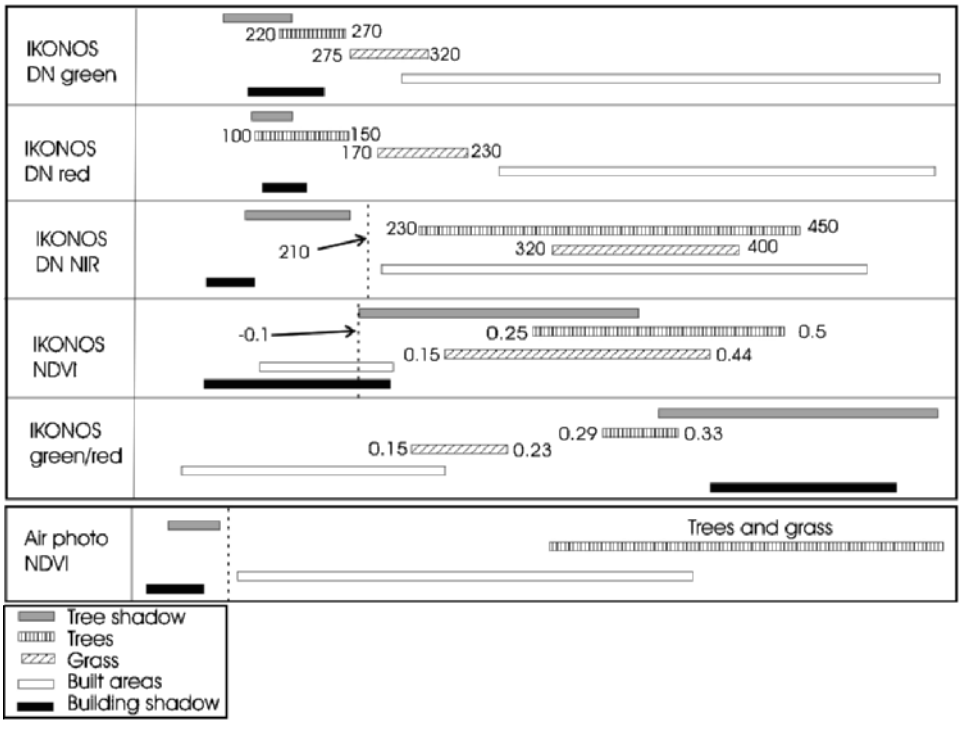

Figure 3. Coincident spectral plots based on two standard deviations above and below the mean, showing threshold used for shadow removal (dashed line), and the relationship between vegetation (trees and grass), built areas and shadows. The numbers represent the pixel values.

105983
International Journal of Remote Sensing res50633.3d 2/11/04 14:07:23
The Charlesworth Group, Wakefield +44(0)1924 369598 - Rev 7.51n/W (Jan 20 2003)

possible in the case of the 11-bit IKONOS data where tree and building shadows are separable spectrally from each other and from other land cover types using a combination of two bands and a semantic filter of the form

$$\text{if } \text{pix}_{\text{NIR}} < 210 \text{ and if } \text{pix}_{\text{NDVI}} > -0.1 \text{ then mean } \text{pix}_{\text{TREECROWN}} \text{ else pix.}$$

This is illustrated by figure 3 where the dashed line indicates the pixel value thresholds in the NIR and NDVI images used in this filter.

The small remaining overlap in the IKONOS NDVI band between tree and building shadow indicated in figure 3 which comprises the lightest 15% of the building shadow was also corrected to the mean value of tree crown. This may not be an over-correction since the shadow of some buildings does obscure vegetation. However herein lies a source of uncertainty in the method for shadow removal.

Using the 8-bit scale of the aerial photographs tree and building shadows are not spectrally separable from each other although they are together separable from other cover types. Thus the first approach was used, allocating the pixel values of both building and tree shadows to null values, which would not be included in the sample plot regressions. This method gave slightly higher correlations than allocating the shadow pixels to the mean value of each sample plot. Figure 4 illustrates the area of shadow corrected on the IKONOS image, which represents 15% of the image area, corresponding to all of the tree shadow and 15% of the building shadow which was changed to the mean value of tree crown.

6. Results

Table 4 indicates that polynomial regression generally produced higher correlations between the field vegetation and image parameters than linear regression. It also shows that for both IKONOS and the aerial photographs, the highest correlations were not obtained for the NDVI. The reasons for these findings are discussed in §8.

Thus, before shadow removal, the best fit between the field plots and image bands are obtained for the IKONOS green/red ratio for vegetation density ($R^2=0.76$) and the red band for vegetation cover ($R^2=0.59$): and for the aerial photographs these were the green/red ratio for vegetation density ($R^2=0.69$) and the red band for vegetation cover ($R^2=0.80$). These images were then processed to remove shadows from the calculations. Following shadow removal the highest correlations for VC were obtained using the red band alone, for both IKONOS and the aerial photographs, with an R^2 of 0.67 for IKONOS, i.e. explaining 67% of the data variability, and 0.82 for the aerial photographs (figure 5(*a*)). For VD the highest correlations were obtained using the green/red ratio with an R^2 value of 0.81 for IKONOS (explaining 81% of the data variability) (figure 5(*b*)) and 0.81 for the aerial photographs (table 4).

The model for regression of VC on the aerial photograph red band ($R^2=0.82$) is:

$$\text{VC} = 9.02 \times 10^{-4}(R) - 0.5(R) + 127.85 \quad (5)$$

The model for regression of VD on the IKONOS green/red ratio ($R^2=0.81$) is:

$$\text{VD} = 13.83(\text{G/R}) + 28.8(\text{G/R}) + 23.52 \quad (6)$$

The *F*-test indicated similarity of the sample variances at the 5% significance level for both VC and VD, suggesting that the regression equations provide good estimates of vegetation cover and density in the study area.

An accuracy test comparing the percentage VD and VC for the 41 field quadrats with the four resulting interpolated maps showed a mean difference within 12.6% for

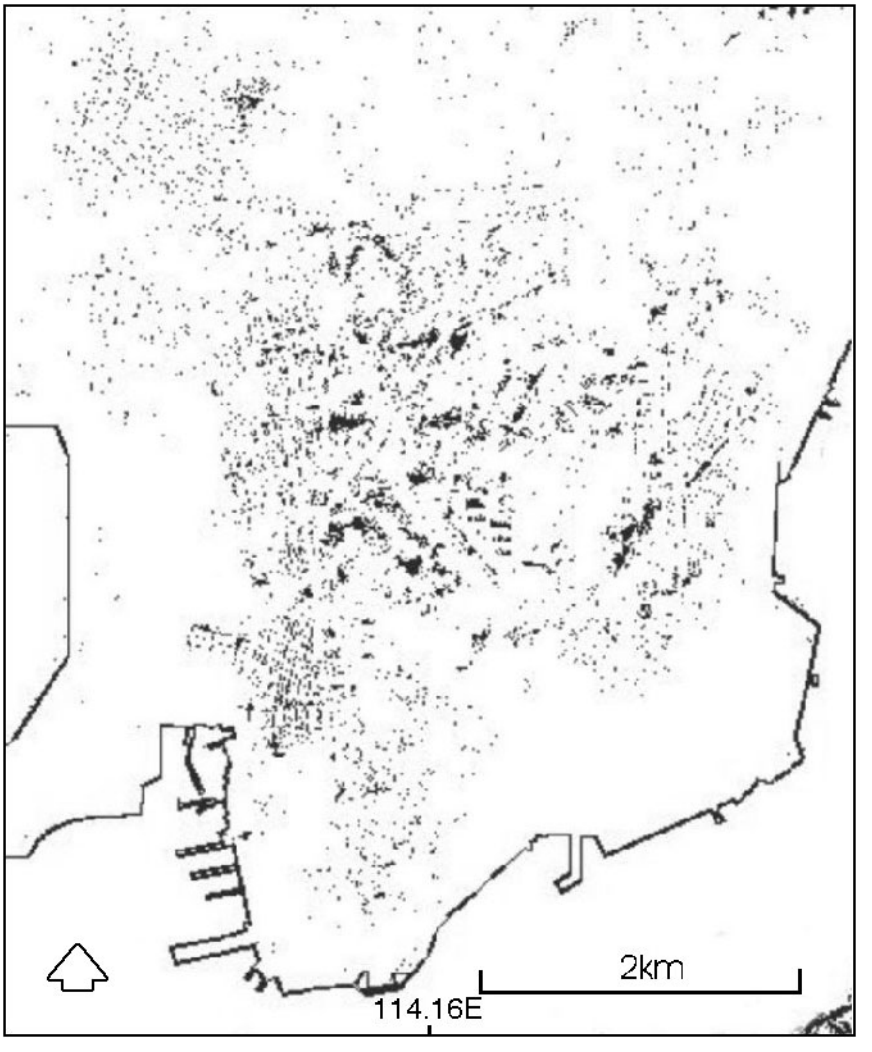

Figure 4. Pixels on the IKONOS image within the range of tree canopy shadow and some building shadow, which were corrected i.e. given the value of tree canopy.

the VC maps and within 5.0% for the VD maps (table 5). The highest agreement (3.8%) was for the VD map produced from the IKONOS green/red ratio. Figure 2 shows the regressed image data for VC figure 2(*a*) and VD figure 2(*b*) displayed as red in FCC images. The grassy runway border at Kai Tak airport projecting into the harbour at right centre illustrates that such areas having high values for VC have low values for VD.

6.1 *Single band versus band ratios*

Table 4 shows that the correlations obtained for the NDVI were generally lower than for both the red and green bands individually, as well as lower than the ratio of green/red. In evaluating the performance of the NDVI Colwell (1974) states that if the reflectance of the soil background is similar to the reflectance of vegetation in a particular waveband then the relationship between reflectance and vegetation

Table 4. Correlations.

(*a*) IKONOS

	Linear regression (R^2)		Polynomial regression (R^2)	
	Cover	Density	Cover	Density
Green	0.36	0.49	0.56	0.73
Red	0.36	0.42	0.59	0.75
NIR	0.13	0.01	0.13	0.42
NDVI	0.16	0.24	0.50	0.61
Green red ratio	0.33	0.55	0.56	0.76
Red shadow removed	0.23		0.67	
Green red ratio shadow removed		0.73		0.81

(*b*) Aerial photographs

	Linear regression (R^2)		Polynomial regression (R^2)	
	Cover	Density	Cover	Density
Green	0.68	0.37	0.82	0.70
Red	0.69	0.26	0.80	0.62
NIR	0.32	0.43	0.60	0.69
NDVI	0.58	0.38	0.65	0.42
Green red ratio	0.55	0.68	0.72	0.78
Red shadow removed	0.69		0.82	
Green Red ratio shadow removed		0.72		0.81

amount will be weak in that waveband. In urban areas in Hong Kong, as in many tropical cities, biomass is contrasted against a generally light-toned background of urban cover types comprising light asphalt, concrete, brick and tile (Akbari 1990), which tend to have high reflectance in both red and NIR bands. In this situation when the background material is light, and vegetative cover low, red energy absorption by vegetation affects the overall response more than reflectance in the green and NIR wavelengths (Colwell 1974). This situation has been encountered using the NDVI in semi-arid rural areas with low vegetation cover, at times other than high summer, where even a negative relationship has been obtained between infrared reflectance and biomass (Boyd 1986, Moleele *et al*. 2001, Xu *et al*. 2002). In 1 the present study the images were obtained in late November, well into the cool dry season, when urban plantings, though still green, are less vigorous. An initial decrease in the NIR reflectance usually precedes decreased red absorption. Figure 3 shows that the reflectance of vegetation in the NIR band is no higher than that of urban surface materials (built areas) but is lower than them in both the green and red bands. Thus although the NDVI shows a distinction between vegetation and built areas, with the built areas being lower, it is not responsive to vegetation amount, and is unable to distinguish between tree cover and grassy vegetation. This is also seen on figure 6(*a*) where trees and grass have a similarly light tone on the NDVI image. It was found that the green and red bands individually, and the green/red ratio, obtained higher correlations between the field vegetation and image parameters than the NIR band or NDVI (table 4). Figure 6(*b*) shows that grass is medium toned on the green/red ratio image compared to the very bright tone of trees. However the green/red ratio was found to be only slightly better than either

International Journal of Remote Sensing res50633.3d 2/11/04 14:07:24 105983
The Charlesworth Group, Wakefield +44(0)1924 369598 - Rev 7.51n/W (Jan 20 2003)

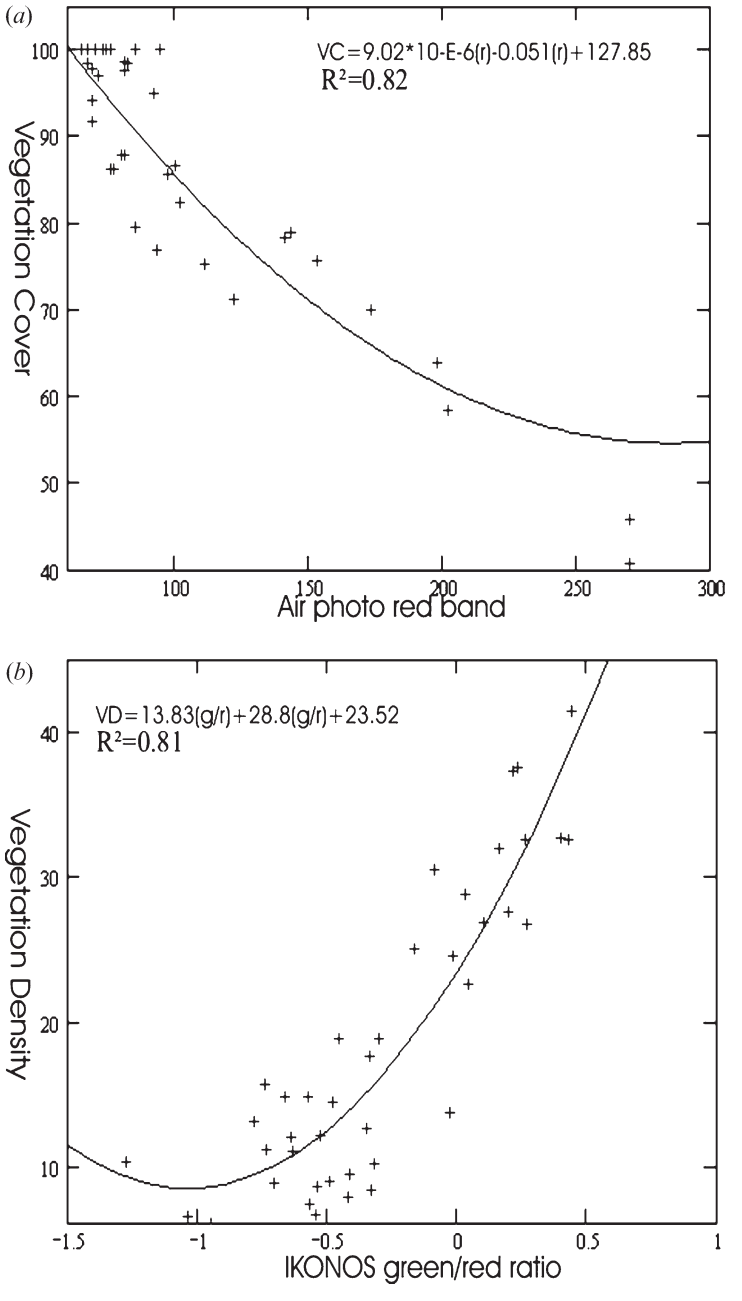

Figure 5. Scatterplots showing polynomial regression of (*a*) air photograph red band on vegetation cover; (*b*) IKONOS green/red ratio on vegetation density.

the green or red band individually, and this only for VD. For VC the red band obtained the best correlation for both sensors.

The high correlation between VC and the red band can be explained by the fact that apart from shadows, vegetation is the darkest feature in the images, due to red energy absorption, contrasted with the high reflectance of urban surface materials. The main reflectance differences between the two biomass parameters VC and VD

Table 5. Summary of highest correlated image bands: mean difference between field vegetation and regressed maps of biomass for 10 test plots.

Image band	Biomass indicator	R^2	Mean difference (%)
IKONOS green/red	Density	0.8	4.0
IKONOS red	Cover	0.67	8.7
Air photograph green/red	Density	0.81	5.2
Air photograph red	Cover	0.82	11.6

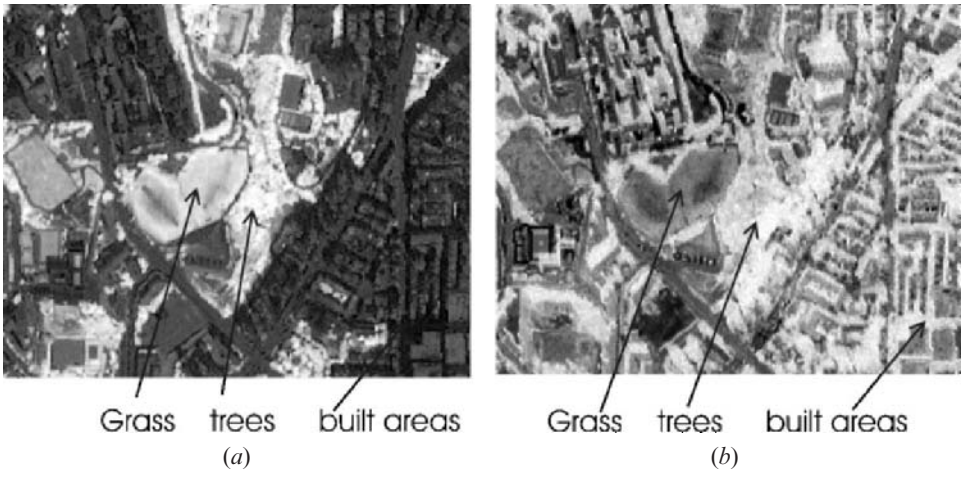

Figure 6. IKONOS ratio images showing two cricket pitches with worn, non-vegetated patches in the centre, adjacent to a forest plot. (*a*) NDVI shows that grass and trees have similarly high values and are not spectrally separable; (*b*) green/red ratio showing that grass and trees are spectrally separable, with grass on the cricket pitch being darker then the trees but brighter than the non-vegetated patches.

result from the recording of a single leaf layer in the case of VC and recording of multiple (overlapping) layers for the VD parameter. Polynomial regression was found to provide the best fit between the field data and image red band for vegetation cover since field plots having high VC, all of which contain large areas of grass cover are not all equally absorptive in the red region, as not all grass may be irrigated in the dry season. Thus, un-irrigated plots on waste ground do not follow the trend of increased red band absorption with increasing cover.

For VD the better correlations obtained using the green/red ratio may be due to the ability of this ratio to represent the greater reflectance in the green band relative to decreased absorption of red wavelengths by a multi-layered canopy, compared with a single canopy i.e. as VD increases the green/red ratio increases and thus green/red has the best separation between grass and trees.

6.2 *The effect of pixel size*

The air photographs, having finer resolution exhibit a wider range of pixel values than IKONOS, being more sensitive to extreme values of biomass. For example the sample plots contain more than 1000 air photograph pixels but only 16–25

IKONOS pixels. Therefore the air photographs containing more pixels with very high or very low biomass should show greater variability than the IKONOS image. The coarser resolution IKONOS image plots would be expected to amalgamate low and high biomass areas within a pixel such that the lower vegetated areas obtain a misleadingly higher biomass value. On the aerial photographs the low and/or highly vegetated areas should have more likelihood of belonging to a pure pixel, having correctly low or high biomass values. The fact that the aerial photographs did not achieve significantly better results than the IKONOS images, despite their superior spatial resolution, especially for VD, may be due to the superior, 11-bit radiometric qualities and absolute radiance values of the IKONOS image bands. Additionally the tree canopies and vegetation patches in the study area are of a similar size order to the 4 m pixels of the IKONOS XS sensor.

6.3 *Effects of shadow removal*

Before shadow removal, some areas within residual primary forest had been mapped as having both low VC and VD values due to large areas of shadow within the tree canopy. Shadows were removed from the sample plots for the highest correlated bands by thresholding the NIR and NDVI bands. The effect was to improve the correlations significantly: thus R^2 increased from 0.76 to 0.80 in the case of VD using IKONOS, and from 0.83 to 0.89 in the case of VC using the aerial photographs (table 4). Furthermore in spite of the smaller pixel size of the aerial photographs whereby shadow areas would more likely comprise a pure pixel, the IKONOS image was more successful in spectrally separating shadows from other cover types probably due to the higher (11-bit) radiometric quality.

7. Application of the findings

In terms of urban environmental quality the total amount of biomass, represented by VD, is a more useful parameter than the total area covered by vegetation represented by VC. Thus trees having high biomass are more important than grass and low shrubs, contributing to environmental quality in terms of aesthetics, air quality, control of pollution, noise and runoff, and habitat provision. On the other hand, the parameter VC may be useful to indicate the total area of open sites and green spaces in cities, or the extent to which an area is not fully built-up. For example, a grassy football field having high VC has low VD, but its presence as an island of green space in a sea of artificial hard surfaces is often significant for aesthetic, climatic and economic reasons, especially in some very densely built high rise districts as found in some parts of Kowloon. Such non-built green areas present opportunities for urban ecological planning within the wider discipline of landscape ecology.

Since the IKONOS image is able to represent VD as accurately as the aerial photographs (R^2=0.8 in each case) planners may utilize IKONOS images for characterizing urban environmental quality by this indicator of vegetation amount. The advantages of using IKONOS over aerial photographs include the empirical nature of the image data in terms of absolute spectral radiance, which can be calibrated for multi-date sensing or over different study areas; the use of a single mapping base with constant geometric and radiometric properties over a large area, and the superior, (11-bit) radiometric resolution. Also, in spite of its coarser spatial resolution IKONOS can show vegetation clearly at single tree level enabling individual street trees to be counted (figure 7) thus permitting precise inventories of

105983
International Journal of Remote Sensing res50633.3d 2/11/04 14:07:25
The Charlesworth Group, Wakefield +44(0)1924 369598 - Rev 7.51n/W (Jan 20 2003)

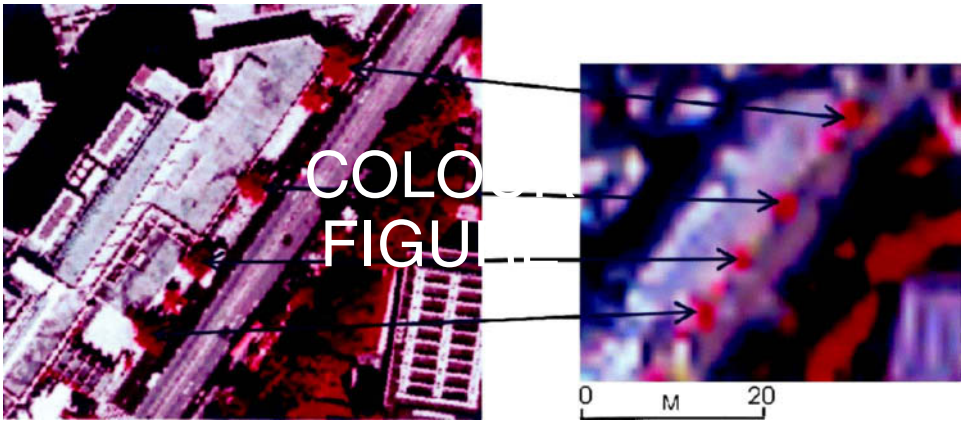

Figure 7. False colour aerial photograph (*a*) and IKONOS image (*b*) showing individual street trees.

street plantings. Additionally cost and manpower requirements for monitoring a whole city are likely to be much lower for IKONOS images than for large scale aerial photographs (table 6). For example manpower requirements involve 4 weeks for data processing using IKONOS compared to 15 weeks using aerial photographs. However, IKONOS obtained significantly lower correlation for VC than the aerial photographs (R^2=0.67 compared with 0.82) and this is believed to be due to the coarser spatial resolution discussed in §6.

8. Conclusion

This research has demonstrated that vegetation in urban areas can be accurately quantified using automated multispectral remote sensing techniques, and that similar accuracy levels can be obtained from IKONOS images and false colour aerial photographs. In the case of vegetation density, the parameter used in this study to indicate biomass amount, IKONOS achieved slightly higher mapping accuracy than the aerial photographs. These promising results were achieved in spite of the fact that the images used did not correspond to the main growing season, when imagery is generally unavailable due to cloud cover. This sub-optimal timing of the images: several weeks into the dry season explains the finding that the NIR band and the NDVI were not the most highly correlated with biomass. The observation that the green and red bands and the green/red ratio all produced higher correlations and more accurate maps than the NDVI is attributed to the fact that

Table 6. Costs of products and manpower ($US) for the whole of Kowloon (50 km^2).

Item	270 infrared aerial photographs	1 IKONOS XS image
Image aquisition	11 538	1 000
Scan digitizing, georeferencing and air photograph mosaicing	11 600 (3 months skilled salary)	2 000 (two weeks skilled salary for georeferencing)
Image processing and production of biomass maps	2 000 (2 weeks skilled salary)	2 000 (2 weeks skilled salary)
Total	25 138	5 000

105983
International Journal of Remote Sensing res50633.3d 2/11/04 14:07:25
The Charlesworth Group, Wakefield +44(0)1924 369598 - Rev 7.51n/W (Jan 20 2003)

senescence first affects the NIR wavelengths with an early collapse of the leaf mesophyll layer reducing the NIR reflectance. Chlorophyll pigments that absorbe strongly in the red wavelengths and weakly in green appear to be the dominant influence on vegetation response in this study. The highly reflecting character of urban surfaces in sub-tropical cities is a further factor mitigating against the use of the NDVI outside the main growing season. Since in the sub-tropics the growing season rarely benefits from clear skies for remote sensing, indices other than the NDVI may prove more useful. However, the NIR and NDVI bands were the most effective for shadow removal due to the greater separability of dark shadows from other features in these bands.

Due to the lack of absolute spectral ranges for the aerial photographs the regression equation derived from them is not applicable to other aerial photographs or study areas. The low (and decreasing) cost of fine resolution satellite imagery such as from Space Imaging's IKONOS and DigitalGlobe's Quickbird may motivate planning departments, even those with free access to air photographs due to government provision, to consider whether the considerable time saved using VHR satellite images warrants a change of techniques.

Acknowledgment

The authors would like to acknowledge funding from the Hong Kong Government CERG grant B-Q611, and the help of an anonymous reviewer.

References

Akbari, H., 1990, Summer heat islands, urban trees and white surfaces. *ASHRAE Transactions*, **96**, pp. 1381–1388.

Barnsley, M.J. and Barr, S.L., 1996, Inferring urban land use from satellite sensor images using kernel-based spatial reclassification. *Photogrammetric Engineering and Remote Sensing*, **62**, pp. 949–858.

Boyd, W.E., 1986, Correlation of rangeland brush canopy cover with Landsat MSS data. *Journal of Rangeland Management*, **39**, pp. 268–271.

Chavez, P.S., 1988, An improved dark-object subtraction technique for atmospheric scattering correction of multi-spectral data. *Remote Sensing of Environment*, **24**, pp. 458–479.

Colwell, J.E., 1974, Grass canopy bi-directional spectral reflectance. *Proceedings of 9th International Symposium on Remote Sensing of Environment,* Ann Arbor, MI, USA, pp. 1061–1085.

Curran, P., 1983, Estimating green LAI from multispectral aerial photography. *Photogrammetric Engineering and Remote Sensing*, **49**, pp. 1709–1720.

Fleming, D., 2003, Ikonos DN value conversion to planetary reflectance. Version 2.1 CRESS Project, Department of Geography, University of Maryland, College Park, MD, USA.

Gao, J. and Skillcorn, D., 1998, Capability of SPOT XS data in producing detailed land cover maps at the urban-rural periphery. *International Journal of Remote Sensing*, **19**, pp. 2877–2891.

Gitelson, A.A., Stark, R., Grits, U., Rundquist, D., Kaufman, Y. and Derry, D., 2002, Vegetation and soil lines in visible spectral space: a concept and technique for estimation of vegetation fraction. *International Journal of Remote Sensing*, **23**, pp. 2537–2562.

Hall, F.G., Strebel, D.E., Nickeson, J.E. and Goetz, S., 1991, Radiometric rectification: toward a common radiometric response among multi-date, multi-sensor images. *Remote Sensing of Environment*, **35**, pp. 11–27.

HANLEY, T.A., 1978, A comparison of line-intercept and quadrat estimation methods of determining shrub canopy coverage. *Journal of Rangeland Management*, **31**, pp. 60–62.

JUSTICE, C.O. and TOWNSHEND, J.G., 1981, Integrating ground data with remote sensing. In *Terrain Analysis in Remote Sensing*, edited by J.G. Townshend (London: Allen and Unwin), pp. 38–58.

KANEMASU, E.T., 1974, Seasonal canopy reflectance patterns of wheat, sorghum and soyabean. *Remote Sensing of Environment*, **3**, pp. 43–47.

LAWRENCE, R.L. and RIPPLE, W.J., 1998, Comparison among vegetation indices and bandwise regression in a highly disturbed, heterogeneous landscape: Mount St Helens, Washington. *Remote Sensing of Environment*, **64**, pp. 91–102.

MOLEELE, N., RINGROSE, S., ARNBERG, W., LUNDEN, B. and VANDERPOST, C., 2001, Assessment of vegetation indexes useful for browse (forage) prediction in semi-arid rangelands. *International Journal of Remote Sensing*, **22**, pp. 741–756.

NOWAK, D.J., ROWNTREE, R.A., MCPHERSON E.G., SISSINI, S.M., KERKMANN, E.R. and SEVENS, J.C., 1996, Measuring and analyzing urban tree cover. *Landscape and Urban Planning*, **36**, pp. 49–57.

SCURLOCK, J.M.O., ASNER, G.P. and GOWER, S.T., 2001, Worldwide historical estimates of Leaf Area Index, 1932–2000. Office of Scientific and Technical Information, Oak Ridge, TN, USA, Report ORNL/TM-2001/268.

SUITS, G.H., 1972, The calculation of the directional reflectance of a vegetative canopy. *Remote Sensing of Environment*, **2**, pp. 175–182.

TUCKER, C.J., 1979, Red and photographic infra-red linear combinations for monitoring vegetation. *Remote Sensing of Environment*, **8**, pp. 127–150.

XU, B., GONG, P. and PU, R., 2002, Crown closure estimation of oak savanna in a dry season with Landsat TM imagery: comparison of various indices through correlation analysis. *International Journal of Remote Sensing*, preview article. 3

105983

International Journal of Remote Sensing res50633.3d 2/11/04 14:07:31
The Charlesworth Group, Wakefield +44(0)1924 369598 - Rev 7.51n/W (Jan 20 2003)

Authors Queries

Journal: **International Journal of Remote Sensing**
Paper: **105983**
Title: **Urban vegetation monitoring in Hong Kong using high resolution multispectral images**

Dear Author
During the preparation of your manuscript for publication, the questions listed below have arisen. Please attend to these matters and return this form with your proof. Many thanks for your assistance

Query Reference	Query	Remarks
1	Xu et al. 2002 – this must be published by now, please update.	
2	Colwell 1974 – publisher and location?	
3	Xu et al. 2002 – this must be published by now, please update.	

105983
International Journal of Remote Sensing **res50633.3d** 2/11/04 14:07:31
The Charlesworth Group, Wakefield +44(0)1924 369598 - Rev 7.51n/W (Jan 20 2003)